Chapter 6
Microstructure of Recycled Aggregate Concrete

6.1 Introduction

Concrete is a composite material which consists of primarily aggregate fragments dispersed in a binding medium (cement matrix). Macrostructure is the gross structure of a material that is visible to the human eye. From the macroscopic examination, the two phases of the concrete can be differentiated easily: cement matrix and aggregates of different shapes and size. Microstructure is the subtle structure of a material that can be resolved with the help of a microscope (Mehta and Monterio 2006). As the concrete is a composite material, the complexities of the microstructure of concrete are evident. It becomes obvious that the two phases of the microstructure are neither homogeneously distributed with respect to each other, nor are they themselves homogeneous. For example, at some places, the hydrated cement paste mass appears to be as dense as the aggregates, while in other places it is highly porous. In the presence of aggregates, the microstructure of hydrated cement paste in the vicinity of large size aggregate is different from the microstructure of the bulk paste. In fact, many aspects of concrete behavior under stress can be explained only when the aggregate–cement paste interface is treated as a third phase of the concrete microstructure (Mehta and Monterio 2006). Thus, the microstructure of concrete has three phases: bulk hydrated cement paste phase, aggregate phase, and the interfacial transition zone (ITZ), which is generally 10–50 μm thick around the aggregate and is generally weaker than the other two phases (bulk cement paste and aggregate) between aggregate particles and cement mortar. Therefore, the ITZ greatly influences the mechanical and durability characteristics of concrete. As the two features of the microstructure of concrete, namely ITZ and hydrated cement paste, are subjected to change with time, environmental humidity, and temperature, the microstructure of concrete is not an intrinsic property of the material.

The interfacial transition zone (ITZ) between the aggregate and the cement mortar matrix is the most important interface in concrete. A fundamental study of this ITZ gives a more insight into the understanding of the concrete characteristics. In general,

M. C. Rao et al., *Systematic Approach of Characterisation and Behaviour of Recycled Aggregate Concrete*, Springer Transactions in Civil and Environmental Engineering,
https://doi.org/10.1007/978-981-10-6686-3_6

the ITZ is the weakest link of the chain and is treated as the strength-limiting phase in concrete (Mehta and Monterio 2006). Therefore, the concrete fails at a considerably lower stress level than the strength of either of the two main components (mortar matrix and aggregate) due to the presence of ITZ. In this composite material (concrete), the ITZ acts as a bridge between the two components, i.e., the coarse aggregate and cement mortar matrix. Even when the individual components are of high stiffness, the stiffness of the composite (concrete) is reduced because of the broken bridges (i.e., voids and microcracks in the ITZ), which do not permit stress transfer. Therefore, the properties of ITZ, especially the porosity and microcracks, have great influence on the stiffness or the elastic modulus of concrete (Mehta and Monterio 2006). In particular, the study of the interface is more important in recycled aggregate concrete, as the recycled aggregate concrete has more interfaces than normal concrete. That is the interfacial transition zone between the original aggregate and the adhered mortar (old ITZ), and another interface between the adhered mortar and new mortar matrix (new ITZ) in recycled aggregate concrete is shown in Fig. 6.1. In contrast, the normal concrete has only one ITZ, i.e., interface between the aggregate and mortar, as can be seen in Fig. 6.2.

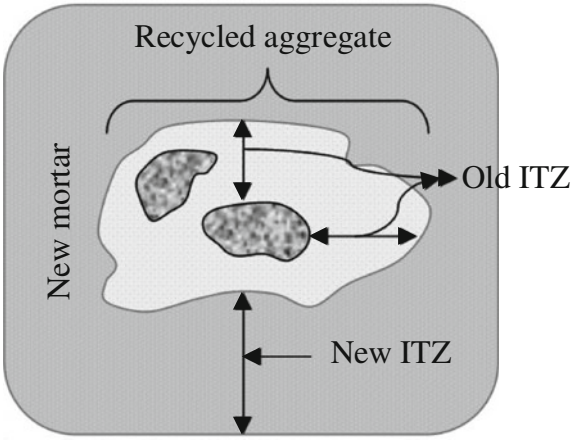

Fig. 6.1 The Interfacial transition zones in RAC

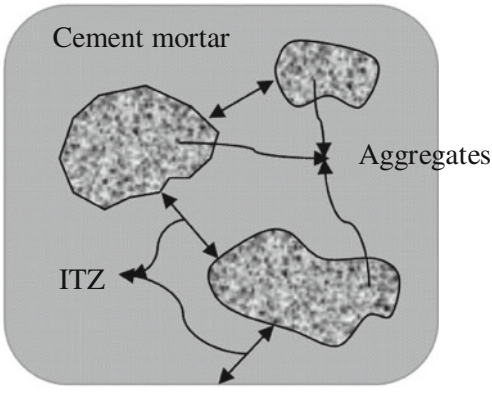

Fig. 6.2 ITZ in normal concrete

It is generally accepted that the cement paste which is adhered to the recycled aggregate is one of the major factors that influence the performance of recycled aggregate concrete. The quality of the mortar and interfaces, as well as the mortar components of the original concrete, thus influences the properties of concrete. The present chapter discusses the characteristics of ITZ in terms of hydration compounds, anhydrous cement, porosity and microhardness, and their influence on the strength of concrete. Further, it discusses the influence of the binder, quality, and quantity of adhered mortar on interfacial transition zone.

Chakradhara Rao (2010) conducted microscopic examination on RAC made with RCA obtained from different sources of RCA. To carry out the microscopic examination, a total of five 100 mm diameter × 200 mm height cylinders each from normal concrete made with type 1 cement (M-RAC0), RAC made with RCA obtained from Sources 1 and 2 (MM-RAC100, MK-RAC100), normal concrete made with type 2 cement (M-RAC0) and RAC made with Source 3 RCA (MV-RAC100) were cast and cured for 28 days along with the samples prepared for the rest of the studies. Both type 1 and type 2 cements belong to OPC 43 grade; however, there is a little difference in their physical, chemical and mechanical properties. In the above mixes, the first letter represents the mix, second letter indicates the Source of RCA (details of Sources are already discussed in Chap. 4), RAC indicates the recycled aggregate concrete, and the number represents the percentage of RCA in the mix.

6.2 Sample Preparation for Microscopic Study

Specimen preparation is very important for identifying the features in scanning electron microscope (SEM). Identification of suitable concrete for microscopic analysis is important due to the complex heterogeneity of concrete. Concrete surfaces with large areas of paste are better suited against those with a lot of aggregate to obtain maximum information. After 28 days of curing, 10–12 mm thick slices were cut from a 100 mm diameter × 200 mm height cylinder at different heights using a precision diamond saw and kerosene as lubricant. From each slice again, approximately 10 × 10 mm rectangular sections were cut. The specimens were then dried in desiccators for more than 3 days. The dried specimens were then vacuum impregnated with a low viscosity epoxy coded as Epoxil-43 and hardener as Epoxil-MH43 in a 3:1 ratio (shown in Fig. 6.3) and allowed to harden at room temperature for 1–6 h.

The importance of the impregnation of the specimens with epoxy resin is to protect the specimen and prevent its damage during subsequent stages of grinding and polishing. In addition, the epoxy resin fills the voids and enhances contrast between the pores, hydration compounds, and anhydrous cement. The impregnated specimens are then carefully grounded and polished. The impregnated specimens are then coarse polished on #500 and #1200 grit paper to remove epoxy from the surface of the specimen. This surface is then subjected to fine polishing on

Fig. 6.3 Test setup for specimen impregnation with low viscosity epoxy resin

automated polishing machine using series of successively finer grade of diamond pastes: 9, 3, 1 and 0.25 μm. Petroleum is used as lubricant during polishing. After every stage of polishing, the specimens are checked under an optical microscope for the quality of polishing achieved. Polishing is then advanced to the next stage and continued till desired level of polishing achieved. Normally, each specimen is polished for 3–4 h to obtain a good surface. The polished specimens are then cleaned in an ultrasonic bath and dried in vacuum to remove any remaining lubricant from the surface. The specimens are then coated with a thin layer of carbon to prevent charging during backscatter scanning electron (BSE) imaging.

6.3 Scanning Electron Microscope (SEM)

The JEOL-JSM-6490 is a high-performance scanning electron microscope with a high resolution of 3.0 nm and is coupled with an energy dispersive X-ray spectrometer (EDS) which is used to analyze the samples in the study. This facilitates the qualitative analysis of the major elements on the surface.

6.4 Image Acquisition

The selection of areas within a given sample, resolution, magnification and the number of images required to acquire are important aspects to be considered during the analysis. To measure the capillary porosity, 800× magnification was appropriate (Sahu et al. 2004). In this study, almost all the backscatter scanning electron (BSE) images are acquired with 1000× magnification at 512 × 512 pixel resolution. Accordingly, each pixel is approximately 0.3 μm in each direction. The basic aim of this study is to characterize the microstructural features (porosity, hydration compounds, and anhydrous cement) of the ITZ. Therefore, each image is selected in

such a way that it covers a small part of the aggregate in addition to the mortar matrix. Similarly, a series of images are acquired randomly along the length of the ITZ. Three samples are considered for each concrete mix, and a total of 20 images are acquired from all the three samples randomly.

6.5 Image Analysis

All the BSE images are analyzed quantitatively by using earth resources data analysis system ERDAS 8.5 image processing software. Depending upon the gray level, intensity 256 classes of shades from black to white are available in the BSE images. Generally, the lowest level, recorded as gray level 0, is fully black and the highest level, recorded as gray level 255, is fully white. In general, darker areas on the image is considered as areas of lower gray level and conversely of the brighter areas as areas of higher gray levels (Diamond 2004). One can easily identify the residual cement from the other components, as the residual cement is at the bright end (fully white) of the gray scale. Similarly, the pores are usually filled with epoxy resin in specimen preparation can accurately be separated from other components, as they are at the dark end of the gray scale. The separation of calcium hydroxide (CH) from the calcium silicate hydrate (C–S–H) is slightly uncertain, as CH is slightly brighter than C–S–H in the gray scale (Diamond 2001). In the present study, based on the gray-level histogram of the BSE images, the threshold values are decided for various components. Nevertheless, in some cases the peak for CH is not clearly visible. One of the histograms of such cases is shown in Fig. 6.4. This may be partly due to the resolution of the BSE technique and partly due to the physical nature of the CH boundary.

The technique adopted in the work of Patel (Scrivener 2004), shown in Fig. 6.5 is used in the present study to fix the arbitrary threshold value for CH.

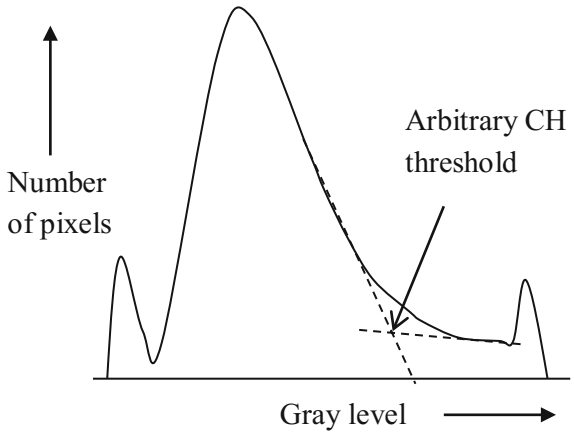

Fig. 6.4 Typical gray-level histogram (from the left, the peaks correspond to pores, C–S–H and anhydrous cement (UH). There is no defined peak for the CH as discussed in the text)

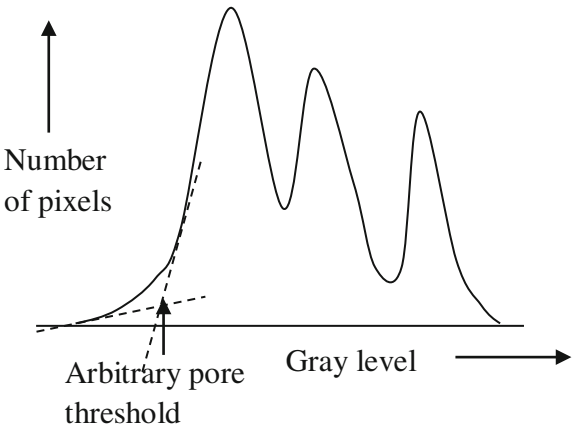

Fig. 6.5 Typical gray-level histogram of hardened cement paste (from the left, the peaks correspond to C–S–H, CH and UH. There is no discrete peak for porosity) (Scrivener 2004)

After finalizing the threshold of each component, the pixels corresponding to each component are separated using binary segmentation. The binary segmentation of some of the images for various components is presented in Figs. 6.6, 6.7, 6.8, 6.9, and 6.10. The percentage area of each component is calculated by dividing the number of pixels of each component by the total number of pixels in the image filed. It is important to mention that the pixels corresponding to aggregate particles are excluded and the percentage area of each component is calculated based on the area of the paste, rather than the area of concrete.

6.6 Vickers Microhardness (HV)

A UHL VMHT microhardness tester (VMH-001) is used to measure the microhardness of ITZ of both normal concrete and recycled aggregate concrete made with all the three Sources of RCA. It has motorized selection of test force which offers full control via touch panel display, and it has the automatic loading procedure. It is interfaced with a computer, which facilitates the easy and accurate measurements of hardness. A typical hardness measurement is shown in Fig. 6.11.

6.7 Characteristics of Interfacial Transition Zone (ITZ)

Interfacial transition zone (ITZ) is the region of cement paste around the aggregate particles, which is perturbed by the presence of aggregate (Scrivener et al. 2004). Due to the large differences between the sizes of aggregates and cement grains, each aggregate particle acts as a mini “wall”, which interrupts the packing of the cement grains. This gives a zone, closest to the aggregate, and contains predominantly

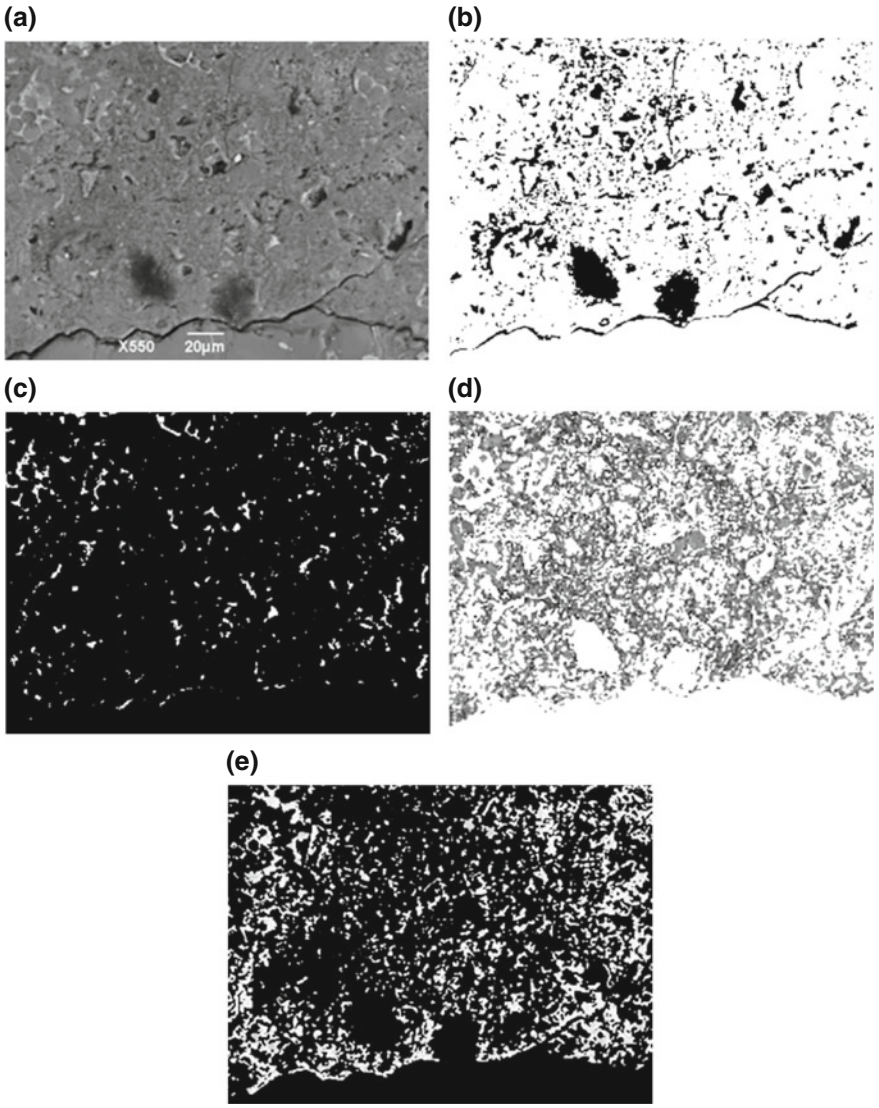

Fig. 6.6 Binary segmentation of BSE images in M-RAC0. (**a**) Gray image (**b**) binary image of pores (**c**) binary image of residual cement (**d**) binary image of C–S–H and (**e**) binary image of CH (Chakradhara Rao 2010)

smaller grains of cement particles and has a significantly higher porosity, while larger cement grains are found to be farther away from aggregate. Due to the deficit of cement grains in ITZ, there is effectively higher w/c ratio initially in this region. Therefore, for a given overall w/c ratio, the w/c ratio in the "bulk" cement paste is comparatively less. In addition, there is a relative movement of paste and aggregate

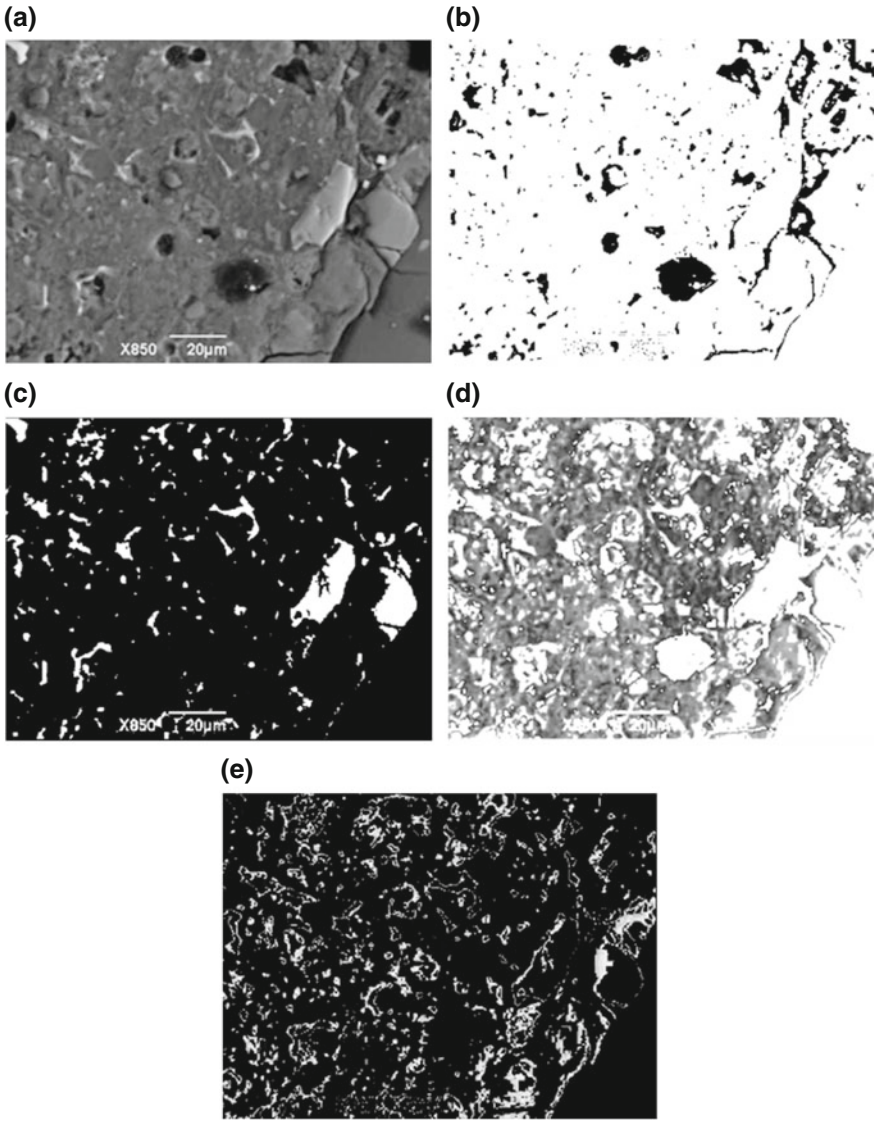

Fig. 6.7 Binary segmentation of BSE images in M-RAC0. (**a**) Gray image (**b**) binary image of pores (**c**) binary image of residual cement (**d**) binary image of C–S–H and (**e**) binary image of CH (Chakradhara Rao 2010)

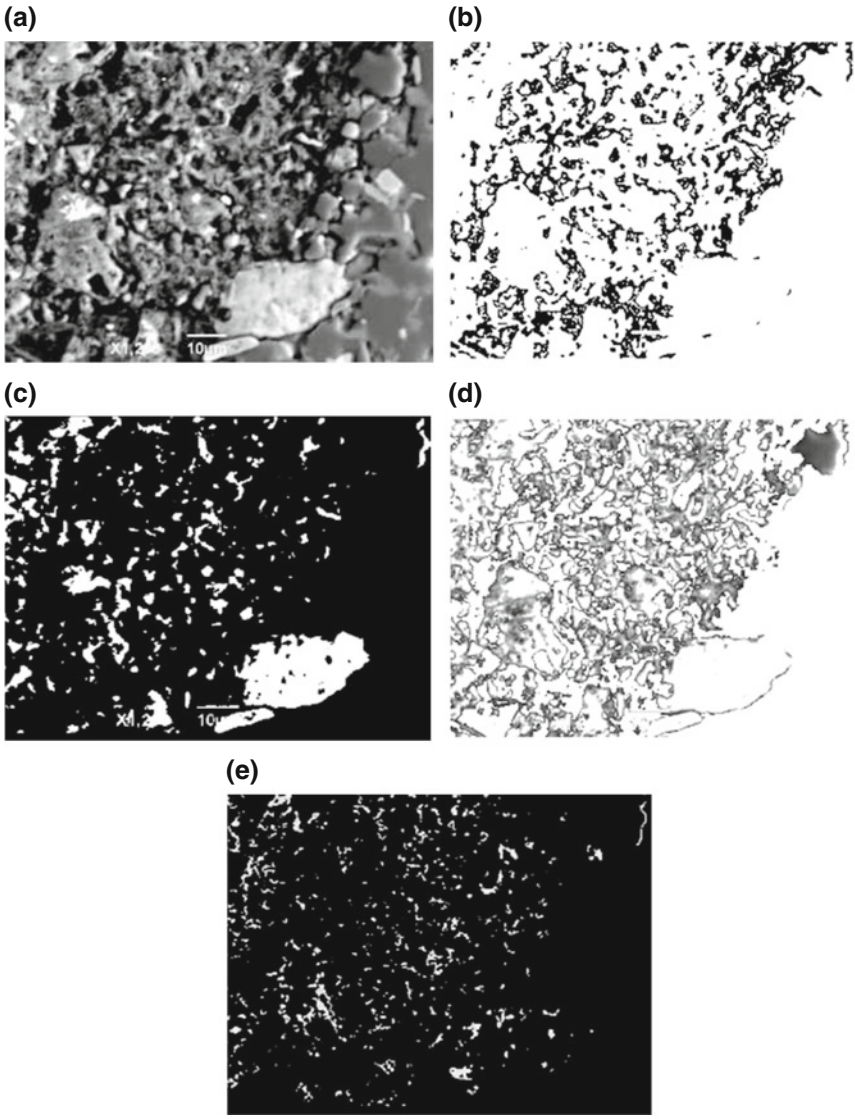

Fig. 6.8 Binary segmentation of BSE image in MM-RAC100. (**a**) Gray image (**b**) binary image of pores (**c**) binary image of residual cement (**d**) binary image of C–S–H, and (**e**) binary image of CH (Chakradhara Rao 2010)

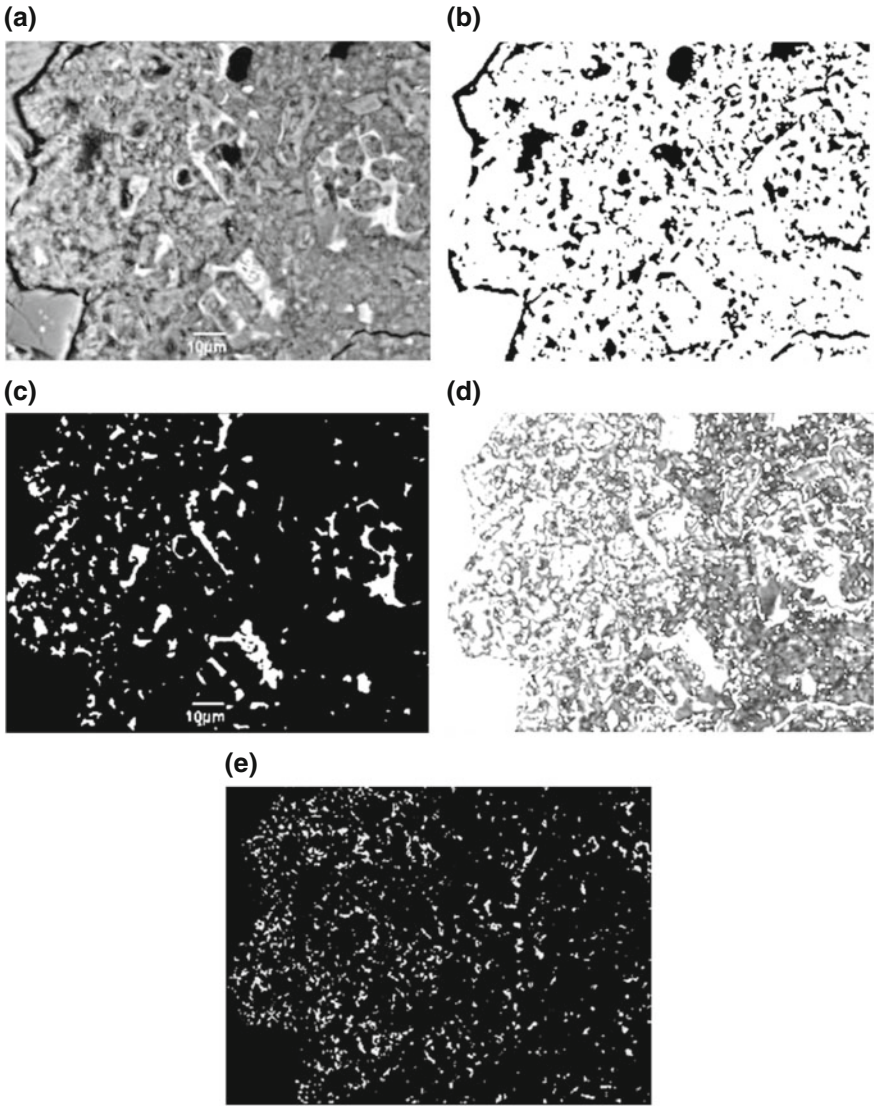

Fig. 6.9 Binary segmentation of BSE image in MK-RAC100. (**a**) Gray image (**b**) binary image of pores (**c**) binary image of residual cement (**d**) binary image of C–S–H, and (**e**) binary image of CH (Chakradhara Rao 2010)

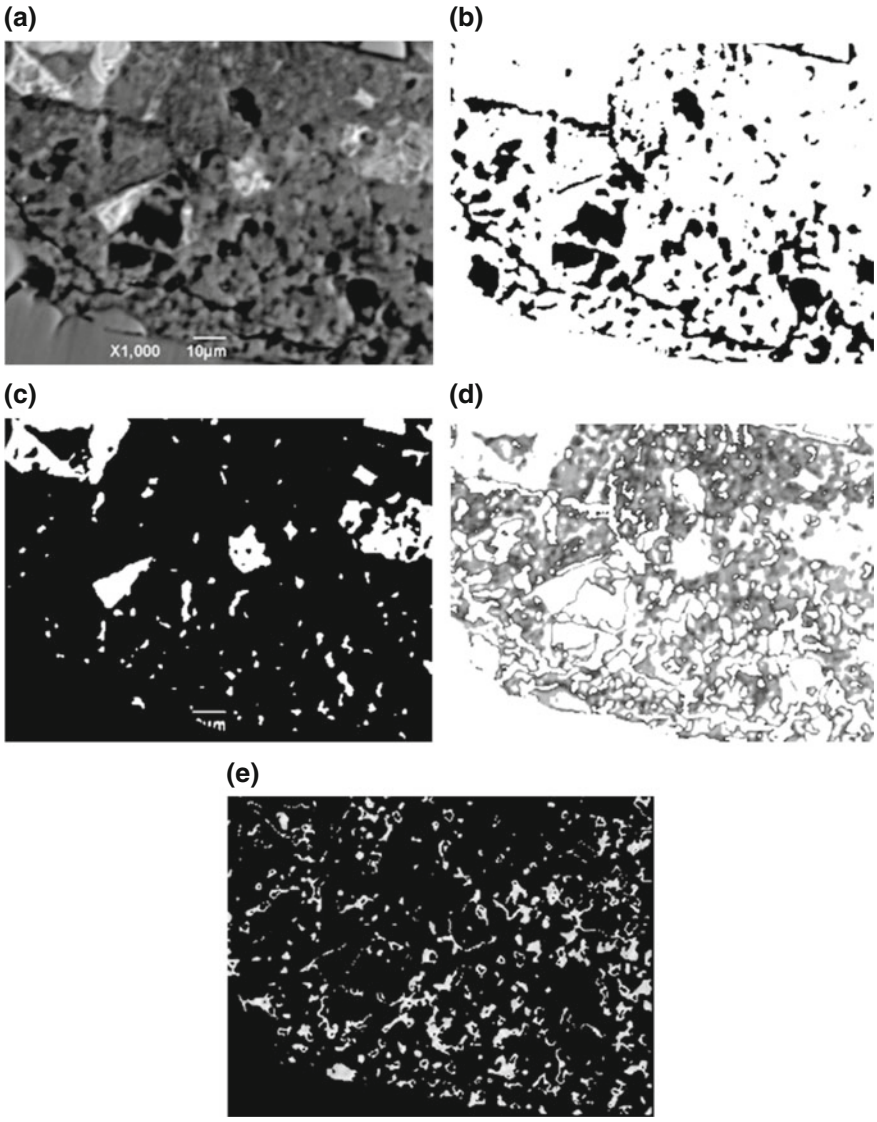

Fig. 6.10 Binary segmentation of BSE image in MV-RAC100. (**a**) Gray image (**b**) binary image of pores (**c**) binary image of residual cement (**d**) binary image of C–S–H and (**e**) binary image of CH (Chakradhara Rao 2010)

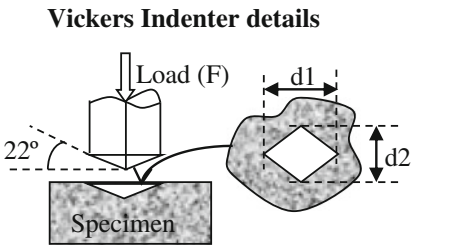

Fig. 6.11 Measurement of Vickers microhardness

particles during mixing. Therefore, the high degree of heterogeneity and relative movement of particles gives large variations in the microstructure of concrete. In the subsequent sections, the important features of ITZ such as hydration compounds, anhydrous cement, and porosity are discussed.

6.7.1 Hydration Compounds, Anhydrous Cement, and Porosity

A large number of BSE images were analyzed using image processing techniques from three samples of each mix (M-RAC0, MM-RAC100, MK-RAC100, M-RAC0, and MV-RAC100) and the percentage area of individual hydration compounds, anhydrous cement, and porosity details are presented in Table A.1 in Appendix A. The mean area percentages of hydration compounds, anhydrous cement, and porosity of both normal concretes and recycled aggregate concretes made with recycled aggregate obtained from all the three Sources are presented in Table 6.1.

Table 6.1 Mean area percentages of porosity and hydration compounds of cement at ITZ (Chakradhara Rao 2010)

Source of RCA	Mix designation	Mean areas of porosity and hydration compounds (%)			
		Porosity	C–S–H + others	CH	UH
Source 1	M-RAC 0	15.22	56.25	18.96	9.57
	MM-RAC 100	20.28	47.94	20.87	10.91
Source 2	M-RAC 0	15.22	56.25	18.96	9.57
	MK-RAC 100	21.02	45.31	21.37	12.72
Source 3	M-RAC 0	16.79	55.41	16.90	10.90
	MV-RAC 100	21.00	49.80	17.67	11.53

It is ascertained that the cement is not fully hydrated in both normal and recycled aggregate concretes after 28 days of curing. This can be observed from the percentage area of remnant unhydrated cement grains (UH) in all the concrete mixes. There are approximately 9.5–11% remnant unhydrated cement grains in case of normal concretes and 11–13% in recycled aggregate concretes. It is also observed that the area percentage of total hydration compounds (calcium hydrate silicate (C–S–H) gel plus other hydrates and CH) is almost same in all the recycled aggregate concretes made with RCA obtained from all the three Sources. Nevertheless, the mean percentage area of total hydration compounds in RAC made with all the three Sources of RCA are less than those of normal concrete. The distribution of individual hydration compounds in normal concrete and recycled aggregate concretes made with recycled coarse aggregate obtained from all the three Sources is presented in Figs. 6.12, 6.13, and 6.14. The C–S–H gel is one of the major hydration

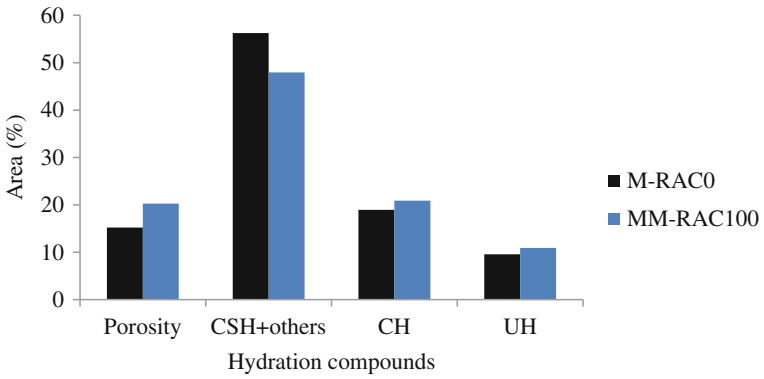

Fig. 6.12 Percentage area of porosity and hydration compounds in ITZ and in bulk paste in both normal concrete and RAC made with Source 1 RCA (Chakradhara Rao 2010)

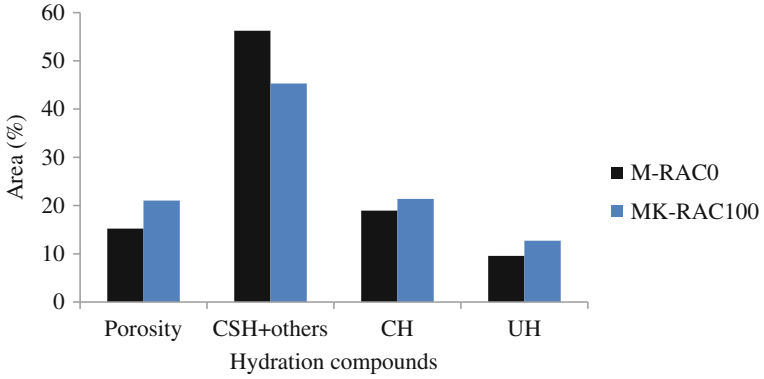

Fig. 6.13 Percentage area of porosity and hydration compounds in ITZ and in bulk paste in both normal concrete and RAC made with Source 2 RCA (Chakradhara Rao 2010)

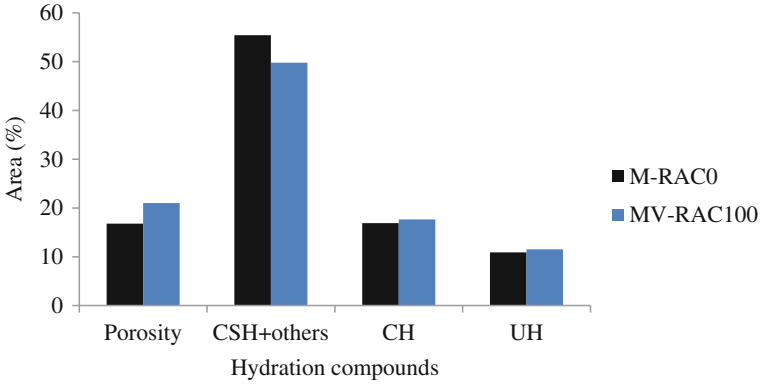

Fig. 6.14 Percentage area of porosity and hydration compounds in ITZ and in bulk paste in both normal concrete and RAC made with Source 3 RCA (Chakradhara Rao 2010)

compounds which contribute to the strength of concrete. It is a form of gel which binds the cement mortar and aggregate and enhances the density of ITZ (Tasong et al. 1998 and 1999). Generally in the initial stages of hydration, the C–S–H gets deposited directly around the cement grains, and in contrast, the calcium hydroxide (CH) mainly gets deposited in the open pores (Scrivener et al. 2004).

The percentage area of gel depends mainly on the ratio of the presence of calcium and silica in the cement and the aggregate type. The percentage area of C–S–H, CH, and UH in RAC made with RCA obtained from the Sources 1 is 47.94, 20.87, and 10.91, respectively, against to those of 56.25, 18.96, and 9.57 in corresponding normal concrete. The percentage area of C–S–H, CH, and UH in RAC made with RCA obtained from Source 2 is 45.31, 21.37, 12.72, respectively, against to those of 56.25, 18.96, 9.57 in corresponding normal concrete. Similarly, the percentage areas of C–S–H, CH, and UH in RAC made with Source 3 RCA are 49.80, 17.67, 11.53 against 55.41, 16.90, 10.9 in the corresponding normal concrete. These percentages of hydration compounds indicate that the ITZ in case of recycled aggregate concrete made with RCA obtained from all the three Sources is less dense when compared to ITZ in normal concrete. This attributes to the high absorption capacity of old mortar adhered to recycled aggregates in RAC.

Porosity is the volume which has not been filled by the cement grains or by the hydration products. The resolution in backscatter SEM limits the measurement of pore sizes. In the present study, all images are captured at 512 × 512 pixels; each pixel is approximately 0.3 μm in each direction which covers an area of 0.09 μm^2. Therefore, the minimum pore size that can be measured is 0.3 μm, and these are generally called capillary pores. The capillary porosity mainly depends on the rate of hydration and w/c ratio. The capillary porosity in matured concrete with a w/c ratio of 0.65 is four times higher than that in concrete with w/c ratio of 0.4 (Sahu et al. 2004). It is observed from Table 6.1 and Figs. 6.12, 6.13, and 6.14, the

porosity in recycled aggregate concrete made with RCA obtained from all the three Sources are more than those of corresponding normal concretes. The area of porosity in normal concrete is in the range of 15.22–16.7%. Whereas, the porosity in RAC made with RCA obtained from Sources 1, 2, and 3 are 20.28, 21.02, and 21%, respectively. Albeit there are some chemical reactions expected between the remnant cement particles in recycled aggregates and new cement mortar would create some interfacial bonding effects, the results indicates that the ITZ in recycled aggregate concrete is loose and porous than normal concrete ITZ. This may be due to the presence of old mortar in recycled aggregates, which absorbs more water during the initial stages of mixing and leads to the higher porosity. The high porosity and water absorption capacity of recycled aggregates made from normal strength concrete coupled with its low initial water content rendered the aggregate to take up a larger amount of water during the initial stages of mixing and hence the open and loose ITZ in RAC (Poon et al. 2004).

6.7.2 *Distribution of Hydration Compounds, Anhydrous Cement, and Porosity Across the Width of ITZ*

As discussed earlier, due to "wall" effect, there is a deficiency of cement grains near the aggregate surface zone. Therefore, there is a substantially higher porosity than the bulk paste. Also, there is a change in the degree of hydration compounds in this zone compared to the bulk paste due to the mobility of hydration compounds. This zone is extended about 30 μm from the aggregate surface (Diamond 2001). As there is a change in the quantities of hydration compounds, anhydrous cement, porosity across the width of ITZ and bulk paste, this section describes how these components distribution differ from ITZ to the bulk paste. To analyze these distributions, each BSE image is segmented into series of strips of each 10 μm wide parallel and along the ITZ. Based on the intensity of gray level, each gray-level image strip is converted into binary image to calculate the quantities of hydration compounds, anhydrous cement grains, and porosity. The original gray-level image, the segmentation and the binary images of various compounds are presented in Figs. 6.15 and 6.16. For each mix, three BSE images are considered and the average results are reported in Table 6.2 (percentage area of each component for each image is presented in Tables A.2–A.6 in Appendix A). The distribution of these components along the length and across the width of ITZ for both normal concrete and recycled aggregate concrete made with RCA obtained from all the three Sources are presented in Figs. 6.17, 6.18, 6.19, 6.20, and 6.21. It is clearly observed that even after 28 days of curing, the cement is not hydrated fully in both normal concrete and recycled aggregate concrete made with all the three Sources of RCA. The gradients of percentage area of anhydrous cement clearly exhibit the wall effect near the aggregate face, i.e., the deficiency of cement grains. The gradients of the percentage area of residual cement grains starting from the aggregate surface

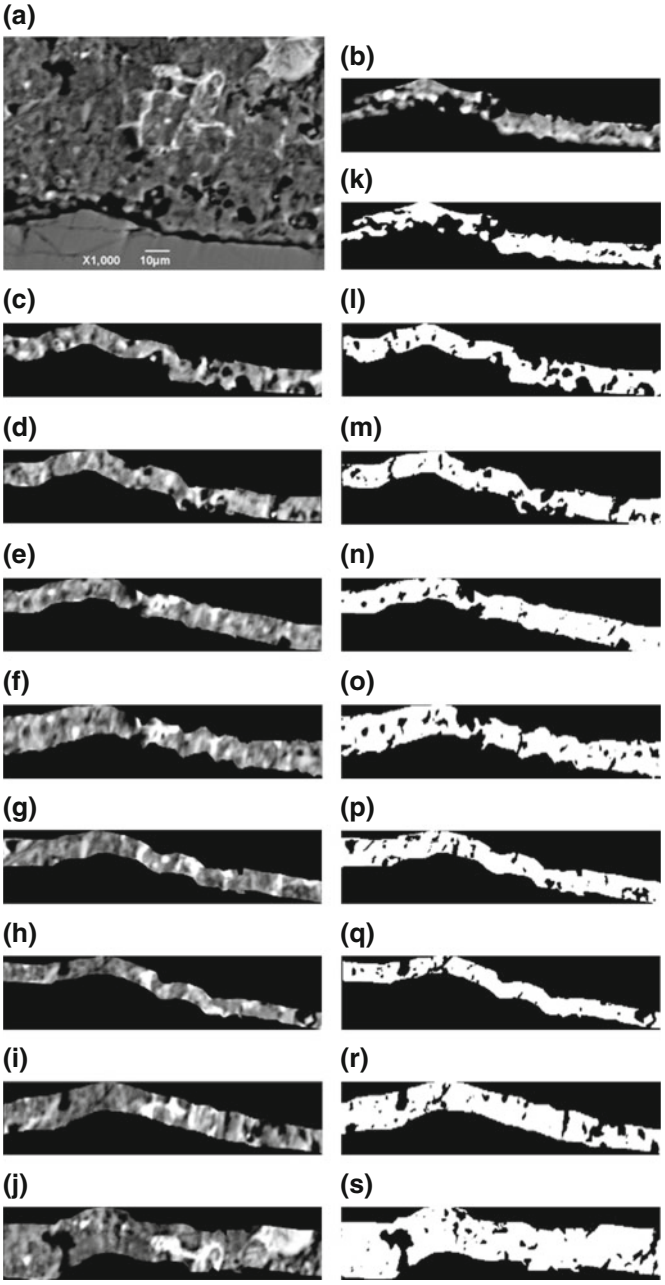

Fig. 6.15 Binary segmented images showing the distribution of pores across the ITZ from aggregate surface (**a**) Gray image (**b–j**) are gray images of 10–80 μm distance from aggregate of each 10 μm width (**k–s**) the pore binary images corresponding to (**b–j**) gray images (Chakradhara Rao 2010)

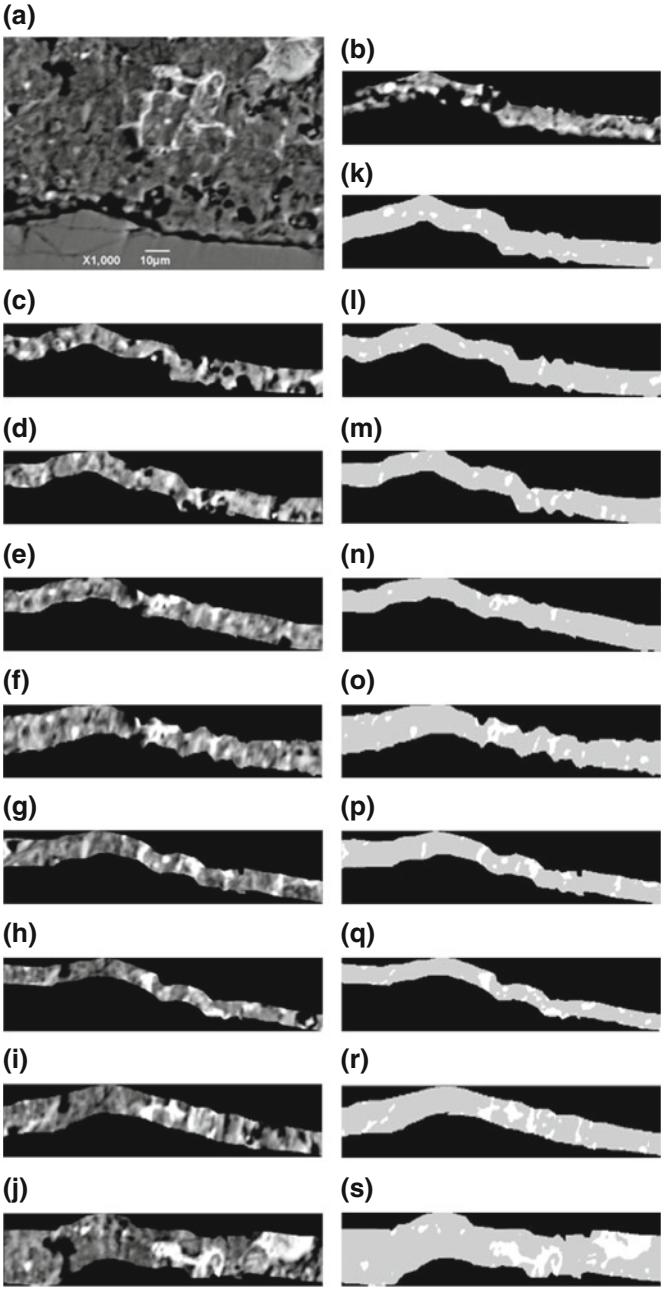

Fig. 6.16 Binary segmented images showing the distribution of residual cement across the ITZ from aggregate face. (**a**) Gray image (**b–j**) are gray images of 10–80 μm distance from aggregate of each 10 μm width (**k–s**) the residual cement binary images corresponding to (**b–j**) gray images (Chakradhara Rao 2010)

Table 6.2 Average percentage area of microstructural constituents of ITZ (Chakradhara Rao 2010)

Source of RCA	Mix designation	Constituent (area percentage)	Distance from aggregate interface (μm)								
			10	20	30	40	50	60	70	80	100
Source 1	M-RAC0	Porosity	21.63	17.70	17.57	16.78	17.71	17.35	16.03	13.82	13.29
		C–S–H + others	45.81	52.84	53.12	55.84	52.77	55.35	56.86	61.45	62.41
		CH	30.23	25.66	24.13	22.13	23.19	20.23	19.46	15.66	13.92
		UH	2.34	3.80	5.18	5.25	6.33	7.07	7.66	9.08	10.38
	MM-RAC100	Porosity	26.34	21.96	20.77	19.80	19.79	19.77	18.34	18.58	19.73
		C–S–H + others	44.93	49.03	51.83	53.54	53.55	53.95	56.38	55.31	55.72
		CH	25.40	23.51	20.66	17.81	17.20	16.50	14.64	15.44	13.82
		UH	3.33	5.50	6.73	8.85	9.46	9.79	10.64	10.67	10.72
Source 2	MK-RAC100	Porosity	26.74	25.41	18.99	19.47	18.02	17.63	16.87	16.61	16.36
		C–S–H + others	44.46	47.09	52.49	54.04	53.45	54.26	56.78	57.67	57.23
		CH	21.99	20.91	20.93	18.19	20.07	19.25	15.88	14.45	14.74
		UH	6.80	6.58	7.59	8.30	8.45	8.86	10.47	11.27	11.67
Source 3	M-RAC0	Porosity	22.59	18.87	17.99	13.73	14.16	14.65	13.30	13.30	15.20
		C–S–H + others	52.47	55.90	58.98	62.85	62.19	60.85	62.79	61.23	59.72
		CH	21.11	20.23	17.29	17.48	16.37	16.79	14.94	15.75	15.49
		UH	3.83	5.00	5.74	5.94	7.28	7.71	8.97	9.71	9.59
	MV-RAC100	Porosity	28.69	24.44	21.54	19.87	18.66	18.39	18.39	16.71	17.67
		C–S–H + others	42.44	47.24	51.70	52.97	54.74	54.82	56.05	58.11	57.72
		CH	21.85	21.07	19.24	19.01	16.48	16.18	14.93	14.38	14.62
		UH	7.02	7.26	7.52	8.15	10.12	10.60	10.62	10.80	9.99

indicate that the residual cement is increasing progressively as the bulk paste approached in both normal concrete and recycled aggregate concrete made with all the three Sources of RCA (also can be seen in Fig. 6.16).

From Fig. 6.17, it is ascertained that the percentage area of residual cement in the first 10–20 μm distance from the aggregate surface is approximately 1/3 of that of the corresponding bulk paste in normal concrete. Whereas, in RAC made with RCA obtained from all the three Sources, the percentage area of anhydrous cement in this zone is approximately 1/2 of that of the corresponding bulk cement pastes (Figs. 6.18, 6.19, 6.21). Beyond 50 μm distance from the aggregate surface, the percentage area of residual cement is almost same in both normal concrete and recycled aggregate concrete. This indicates that the percentage area of UH in the first 10–20 μm zone in RAC is more than that of normal concrete. Similar results are reported in the literature for normal concrete made with dolomite sand and coarse aggregate at 3 days curing (Diamond and Huang 2001). This may be

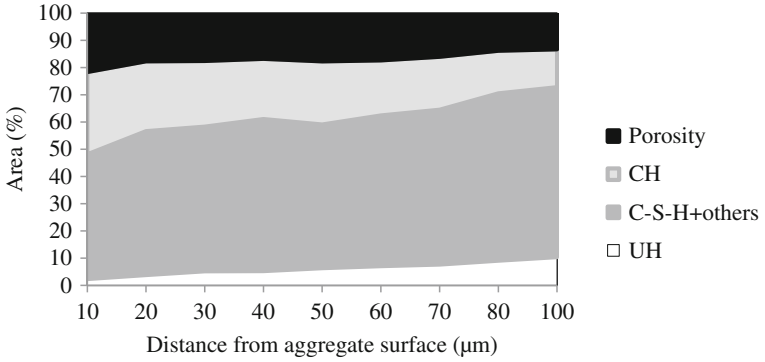

Fig. 6.17 Average distribution of microstructural constituents at the interfacial transition zone (ITZ) in normal concrete (Sources 1 and 2) (Chakradhara Rao 2010)

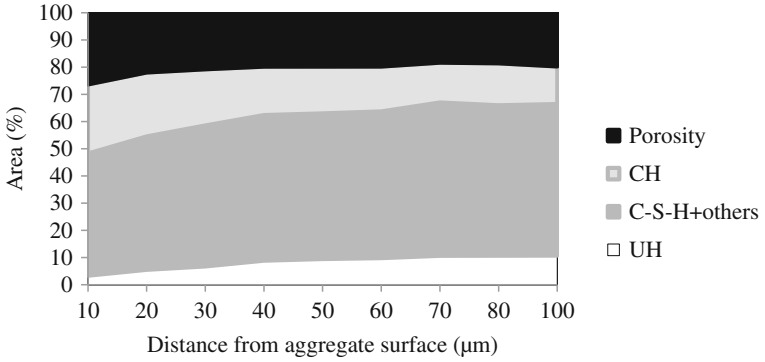

Fig. 6.18 Average distribution of microstructural constituents at the interfacial transition zone (ITZ) in MM-RAC100 (Source 1) (Chakradhara Rao 2010)

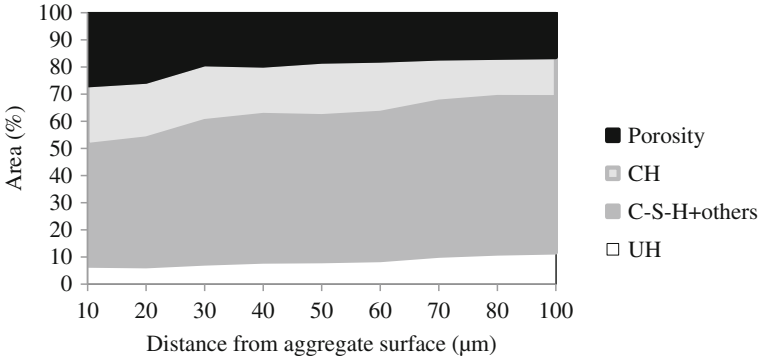

Fig. 6.19 Average distribution of microstructural constituents at the interfacial transition zone (ITZ) in MK-RAC100 (Source 2) (Chakradhara Rao 2010)

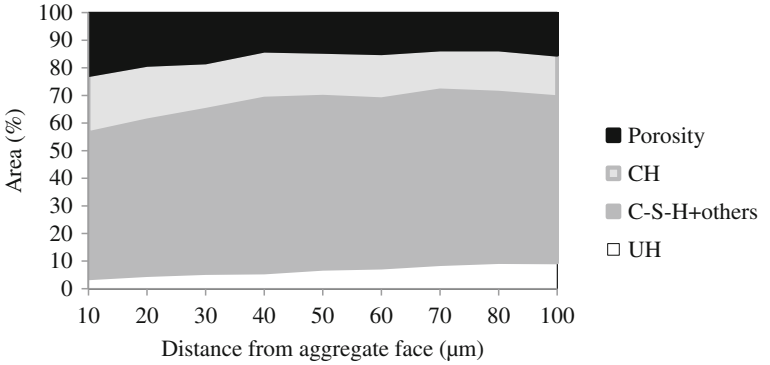

Fig. 6.20 Average distribution of microstructural constituents at the interfacial transition zone (ITZ) in normal concrete (Source 3) (Chakradhara Rao 2010)

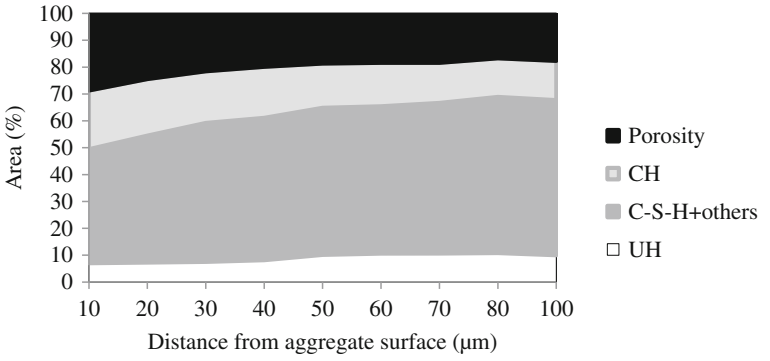

Fig. 6.21 Average distribution of microstructural constituents at the interfacial transition zone (ITZ) in MV-RAC100 (Source 3) (Chakradhara Rao 2010)

attributed to the adherence of old cement mortar to RCA in RAC. Due to high absorption capacity of old cement mortar which is adhered to RCA, the net available water for hydration of new cement grains in this zone is less when compared to normal concrete. The percentage area of UH in the first 10–40 μm zone is around 8.15–8.85% in RAC made with RCA obtained from all the three Sources of RCA against a value of 5.25–5.94% in corresponding normal concrete. With respect to the gradient of anhydrous cement, the effective width of ITZ may be approximately 40–50 μm. Scrievener and Pratt (1996) ascertained from the gradient of anhydrous cement of a one year cured concrete the effective width of interfacial transition zone is at least 50 μm confirming the long-range effect of the aggregate "wall" on the packing of cement grains. Diamond and Huang (2001) found that the effective width of ITZ was 50 μm or more.

Calcium hydroxide (CH) and calcium silicate hydrates (C–S–H) are the major hydration compounds of the cement. The C–S–H directly gets deposited around the cement grains and calcium hydroxide directly gets deposited in pores. The gradients of the percentage areas of C–S–H and CH in normal concrete and recycled aggregate concretes are depicted in Figs. 6.17, 6.18, 6.19, 6.20, and 6.21. It is observed from the figures that, the C–S–H increases as the distance increased from the aggregate surface to the bulk paste in both normal and recycled aggregate concretes. In contrast, starting from the aggregate surface, the CH progressively decreased as the bulk paste approached. In the first 0–40 μm distances from the aggregate surface, the percentage area of CH in normal concrete is relatively higher than that of RAC made with RCA obtained from all the three Sources. This indicates that there is relatively more deposits of calcium hydroxide in the zone nearby aggregate in case of normal concrete compared to recycled aggregate concretes. Similarly, the figures clearly show that there is a relatively higher deposit of C–S–H in case of normal concrete compared to RAC. These deposits of hydration compounds improve the ITZ density. Therefore, the ITZ of normal concrete is relatively dense than those of RAC. This may be mainly due to the presence of old mortar in RCA, which consumes more water during the initial period of mixing leading to less water for hydration at the ITZ in case of RAC. Beyond 20 μm distance from the aggregate surface to the bulk paste, the percentage area of C–S–H is almost identical in both normal concretes and recycled aggregate concretes made with all the three Sources of RCA. Similar results are reported in the literature for 3-day old and 100-day old well-mixed concretes made with dolomite aggregate, in which the authors found that the area percentage of C–S–H was almost identical throughout the concrete (Diamond and Huang 2001). It indicate that within the aureole the quantity of C–S–H formed from the limited content of cement locally available is supplemented by C–S–H derived from the cement rich areas outside of the aureole.

As there is a large difference between the sizes of aggregate particles and cement grains, each aggregate particle acts as a mini "wall" which interrupts the cement grains packing, resulting in the wall effect (Scrivener et al. 2004). As a result of this, the preponderance of small size cement grains at near the aggregate surface has a significantly higher porosity, whereas larger particles of cement grains being further out. In other words, due to this wall effect near the aggregate surface (around

15 μm), less cement grains are present in the fresh state. This is equivalent to a higher w/c ratio. In a typical concrete, some 20–30% of the cement paste lies within 15 μm of aggregate. Therefore, a higher w/c ratio in this zone means that the w/c ratio of the bulk paste is reduced. For a concrete with an overall w/c ratio of 0.4, the w/c ratio of the bulk paste is only around 0.35 (Scrivener et al. 2004). The distribution of the porosity in both normal concrete and recycled aggregate concretes made with recycled coarse aggregates obtained from all the three Sources is presented in Figs. 6.17, 6.18, 6.19, 6.20, and 6.21. It indicates that the percentage area of porosity decreased progressively with the increased distance from the aggregate surface to the bulk paste in all the concretes. In addition, it is observed that a relatively high-percentage area of porosity lies within the first 20 μm distance from the aggregate surface compared to the bulk paste region in both normal and recycled aggregate concretes. The percentage area of porosity in the first 10 μm zone from aggregate in RAC made with RCA obtained from the Sources 1 and 2 is 26.34 and 26.74, respectively, against 21.63% in the corresponding normal concrete. Similarly, the percentage area of porosity in RAC made with Source 3 RCA is 28.69 compared to a value of 22.59 in the corresponding normal concrete. Scrivener et al. (2004) have reported similar results for normal concrete in the literature, in which the authors ascertained that the percentage volume of porosity adjacent to the interface was 40% more than that in the bulk at the time of mixing. After one day, the porosity was reduced to only 10–20% and the slope is less steep. In addition, the authors ascertained that the area percentage of porosity at the ITZ and in bulk paste reduced almost equally at larger period of curing and the results are reported in Fig. 6.22. These results indicate that the ITZ in RAC is less dense and more porous than those of the corresponding normal concretes. In recycled aggregate concrete, though there may be some additional hydration compounds developed due to the reactions between old cement mortar adhered to RCA and new cement matrix, still the percentage area of porosity is higher.

As the recycled aggregates absorb more water, the net water available for hydration of cement is reduced at the initial stages of mixing, which leads to higher

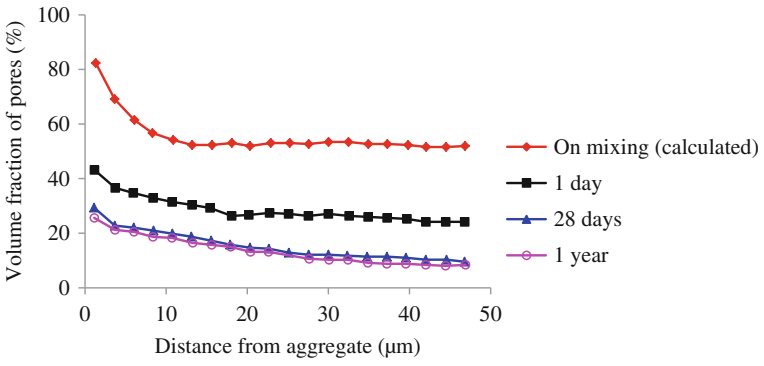

Fig. 6.22 Average porosity in ITZ at various ages (Scrivener et al. 2004)

porosity. The gradients of the percentage area of porosity of RAC made with all the Sources of RCA are relatively steeper than those of corresponding normal concretes after 20 μm distance from the aggregate. This indicates that the effective width of ITZ is more in case of RAC than normal concrete. As discussed earlier, the total aggregate–cement ratio is less in case of RAC mixes compared to normal concrete mixes due to lower specific gravity of RCA, these further allows the rearrangement of cement grains over greater distances resulting in wider interfacial zones. Low water–cement ratios and high aggregate–cement ratios give dense packing of cement grains at the aggregate and minimize the width of interfacial transition zone (Scrivener and Pratt 1996).

6.7.3 *Effect of Aggregate*

Gradet and Ollivier ascertained that the mineralogy of the aggregate influences the degree of orientation of calcium hydroxide (CH) in the interfacial transition zone (Scrivener and Pratt 1996). Whereas, Crumbie (1994) found that the influence of type of aggregate on microstructural gradients analyzed by image analysis was relatively less in real concretes. The EDS analysis of both natural aggregate and recycled coarse aggregates obtained from all the three Sources is presented in Figs. 6.23, 6.24, 6.25, and 6.26, respectively.

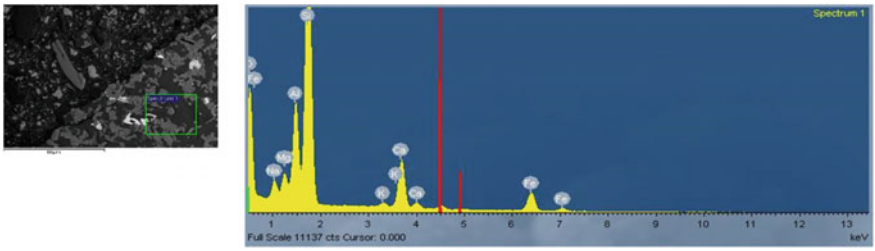

Fig. 6.23 BSE image with EDS analysis of natural coarse aggregate (Chakradhara Rao 2010)

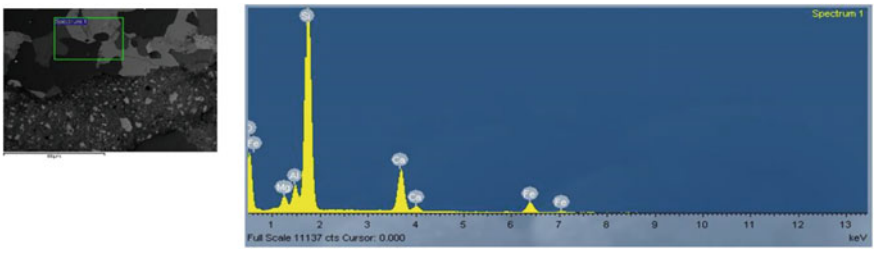

Fig. 6.24 BSE image with EDS analysis of recycled coarse aggregate obtained from Source 1 (Chakradhara Rao 2010)

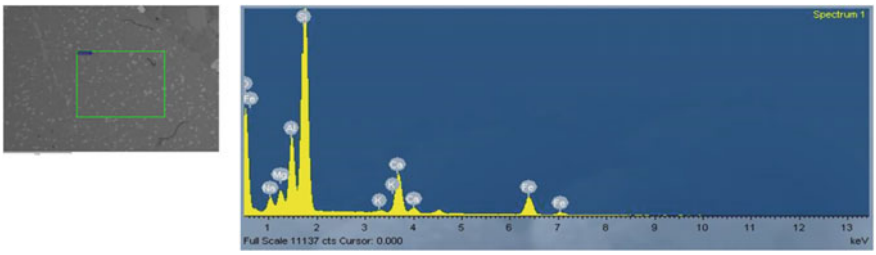

Fig. 6.25 BSE image with EDS analysis of recycled coarse aggregate obtained from Source 2 (Chakradhara Rao 2010)

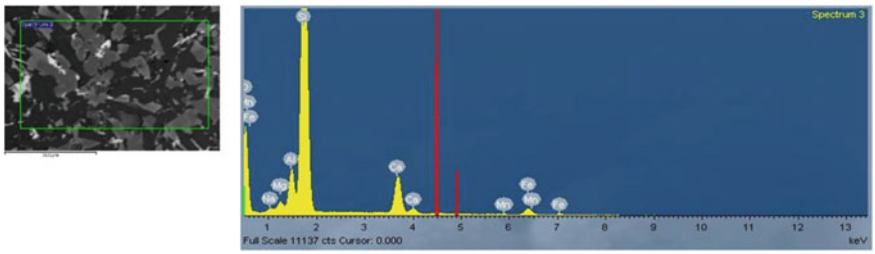

Fig. 6.26 BSE image with EDS analysis of recycled coarse aggregate obtained from Source 3 (Chakradhara Rao 2010)

It is observed that all the aggregates belong to the group of feldspar mineral with the predominant element Si and other elements of Al, Ca, Na, and Fe. Even though the basic mineralogy of both natural and recycled aggregates is similar, the surface texture of recycled aggregate is rough and porous due to the adherence of old mortar which may affect the width of ITZ. The rougher surface attracts the more number of smaller size cement particles, and there may be some additional hydration products due to the reactions between old and new cement mortars which may further improve the ITZ. However, in the present study, the gradients of ITZ indicate that this effect is not significant, as the porosity is higher in case of RAC than normal concrete.

6.8 Compressive Strength–Porosity Relationship

The compressive strength of both normal concrete and recycled aggregate concrete made with RCA obtained from all the three different demolished structures of different sources are discussed in detial in Chap. 4. The porosity measured in the ITZ and bulk paste of various concretes using image processing techniques are discussed in the previous sections. For better understanding, the compressive

Table 6.3 Compressive strength and porosity of both normal concrete and recycled aggregate concretes (Chakradhara Rao 2010)

Mix designation	Compressive strength (f_{ck}) in MPa	Fraction of porosity
M-RAC0	43.08	0.2028
MM-RAC100	40.08	0.2102
MK-RAC100	45.5	0.21
M-RAC0	55.25	0.1679
MV-RAC100	49.45	0.1522

strength at 28 days and porosity of both normal concrete and recycled aggregate concrete made with all the three Sources of RCA are presented in Table 6.3.

Strength of concrete is influenced by the volume of all voids in concrete (Neville 2006). A Power's model which relates the strength and porosity of bulk cement paste in normal concrete presented in Eq. 6.1 is used in the present study.

$$f_{ck} = f_{c,0}(1-p)^n \tag{6.1}$$

where p is the porosity

f_{ck} is the strength of concrete with porosity p
$f_{c,0}$ is the strength at zero porosity and
n is a coefficient

The relationship between compressive strength (f_{ck}) and porosity (p) is obtained by plotting the compressive strength (f_{ck}) versus (1–p) as shown in Fig. 6.27. A power best fit is assumed and the obtained best-fit equation is expressed as

$$f_{ck} = 98.79 \times (1-p)^{3.598} \qquad (\mathrm{R} = 0.98) \tag{6.2}$$

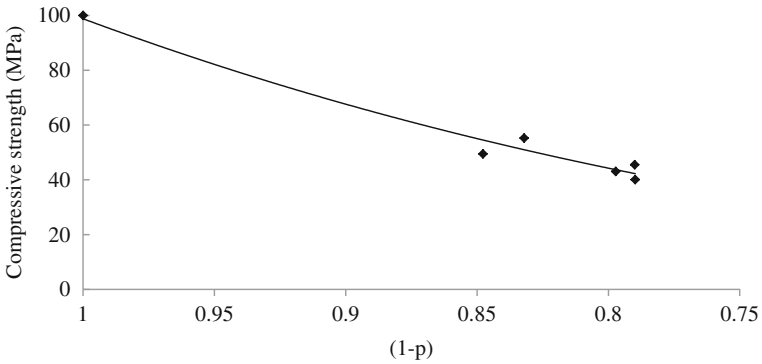

Fig. 6.27 Relationship between compressive strength and porosity (Chakradhara Rao 2010)

This shows that the Power's model given for normal concrete very well matches with the experimental results obtained for both normal concrete and recycled aggregate concretes made with all the Sources of RCA. The intrinsic strength of concrete (corresponding to zero porosity) is 98.79 which is close to the theoretical value of 100.

6.9 Microhardness of ITZ

The microhardness testing has been reported as a means of characterizing the properties of ITZ relative to the bulk and as a means of determining the width of ITZ. The usefulness of this method is its ability to determine the response to load of a volume element that is considerably smaller than the ITZ (Igarashi et al. 1996). The Vickers microhardness test is conducted on the samples on which the BSE images are acquired using scanning electron microscopy. It was reported that in recycled aggregate concrete, there are two ITZs; one is the old ITZ, i.e., ITZ, between original aggregate and the adhesive mortar, i.e., old cement mortar, and the other is between old cement mortar and new cement mortar (new ITZ) (Otsuki et al. 2003). As the new ITZ, i.e., ITZ, between the old cement mortar and new cement mortar could not be identified in the images, the microhardness test is conducted only at old ITZ, i.e., ITZ, between original aggregate and old cement mortar in the present study in case of RAC. The Vickers microhardness is measured at 14 points within the distance of 205 μm from the aggregate surface. The measurements are taken randomly at a constant load of 10 gf with 10 s time. The test is conducted on three samples for each mix, and the average results are reported in Table 6.4. Here the microhardness symbol HV 0.01 means the test load is of 10 gf. The microhardness indentations on various samples are shown in Fig. 6.28.

The distribution of Vickers microhardness across the ITZ for both normal concrete and recycled aggregate concrete made with all the three Sources of RCA is presented in Fig. 6.29.

From the results, it is ascertained that the Vickers microhardness increased with the increase in distance from the aggregate surface in both normal concrete and recycled aggregate concrete made with all the three Sources of RCA. In addition, it is observed that the Vickers microhardness up to 40–55 μm distance from the aggregate surface is not varying much in both normal concrete and recycled aggregate concrete. However, beyond these distances, the Vickers microhardness is progressively increasing up to around 150 μm distances, and thereafter, almost it is constant. Lower value of Vickers microhardness indicates the presence of more microcracks and micropores which is an indication of higher porosity. This variation defines the width of ITZ. The width of ITZ in both normal concrete and recycled aggregate concretes is within the range of 40–55 μm. Similar results are obtained in SEM examinations; the porosity near the aggregate surface (10–50 μm) is much higher than that of bulk paste in all the concretes. The variation in Vickers microhardness of RAC is almost the same irrespective of the Source of RCA.

Table 6.4 Average Vickers microhardness of both normal concrete and recycled aggregate concrete made with RCA obtained from all the three Sources (Chakradhara Rao 2010)

Distance from aggregate surface (μm)	Mix designation			
	M-RAC0	MM-RAC100	MK-RAC100	MV-RAC100
	Vickers microhardness (HV 0.01)			
10	64	45.67	43.00	40.50
25	70	47.00	42.00	43.50
40	72	47.50	49.67	43.00
55	70	58.67	43.00	45.00
70	76	53.50	59.00	50.00
85	85	72.00	52.00	53.33
100	75	62.00	83.50	62.00
115	85	63.00	64.00	53.50
130	76	64.00	74.00	60.50
145	100	62.50	69.00	63.00
160	105	57.50	71.00	67.00
175	109	60.00	70.00	64.00
190	112	62.00	70.00	62.75
205	113	61.00	74.00	63.00

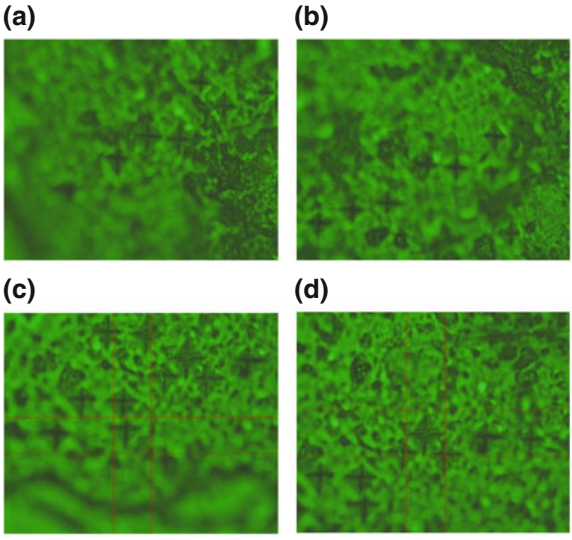

Fig. 6.28 Microhardness indentations of ITZ (**a–b**) normal concrete and (**c–d**) MM-RAC100 (Chakradhara Rao 2010)

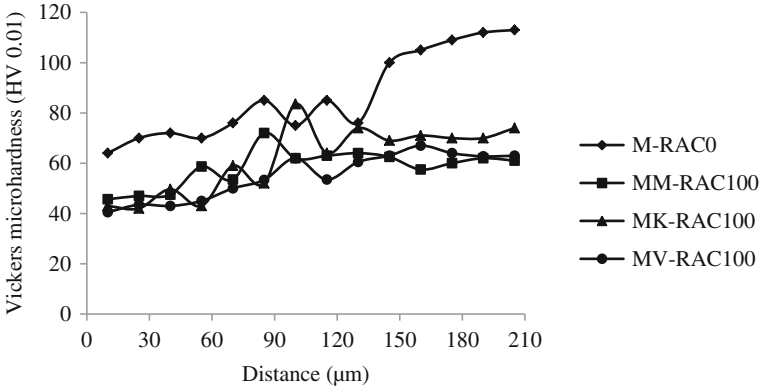

Fig. 6.29 Gradients of Vickers microhardness of both normal concrete and RAC made with all the three Sources of RCA (Chakradhara Rao 2010)

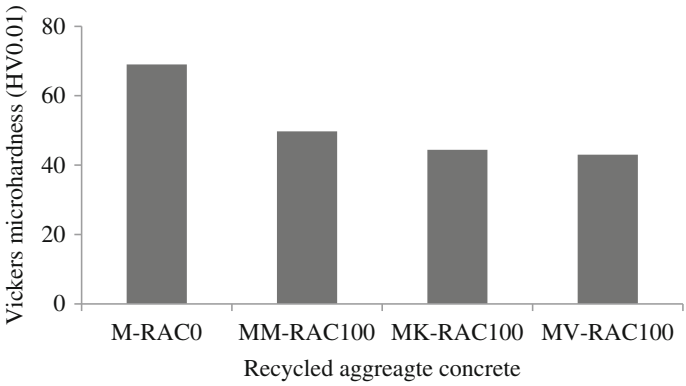

Fig. 6.30 Microhardness of ITZ of both normal concrete and recycled aggregate concretes (Chakradhara Rao 2010)

However, the Vickers microhardness of normal concrete is higher than that of recycled aggregate concretes made with all the Sources of RCA across the ITZ. This may be due to the presence of old mortar adhered to RCA in RAC, which absorbs more water at the initial stages of mixing and leads to the lesser hydration compounds and more porosity.

The ITZ Vickers microhardness is defined as the average value of Vickers microhardness measured within 10–50 μm distance from the aggregate surface (Otsuki et al. 2003). As there is no significant change observed within 10–55 μm distance from the aggregate surface, the width of ITZ is defined as the average Vickers microhardness within 10–55 μm distances from the aggregate surface in the present study. Here microhardness symbol HV 0.01 means the test load is of 10 gf. The Vickers microhardness of ITZ in both normal concrete and recycled

aggregate concrete made with RCA obtained from all the three Sources of RCA is presented in Fig. 6.30. It can be seen that the Vickers microhardness of RAC made with RCA is less than that of normal concrete. The Vickers microhardness of RAC made with RCA obtained from the Sources 1, 2, and 3 is 49.7, 44.4, and 43, respectively, against a value of 69 in normal concrete. Lower values of Vickers microhardness indicate the higher values of porosity and softness of cement paste.

6.10 Compressive Strength–ITZ Microhardness Relationship

The characteristics of ITZ play a major role on the mechanical properties of concrete. The Vickers microhardness is also an indication of the quality of ITZ. Hence, the compressive strength and ITZ Vickers microhardness are related in the plot shown in Fig. 6.31.

The results reported by different researchers for different w/c ratios are also presented. It can be seen that the compressive strength decreases with the decrease in ITZ Vickers microhardness. Lower microhardness indicates higher porosity and hence lowers the strength. Similar trends have been reported in the literature (Otsuki et al. 2003; Ryu 2002).

Ryu (2002) had conducted the experiments on the strength of old and new ITZ in RAC at w/c ratio of 0.55 and 0.25. It was observed that at higher w/c ratio (0.55), the Vickers microhardness of old ITZ is higher than the Vickers microhardness of new ITZ, and at lower w/c ratio (0.25), the Vickers microhardness of new ITZ is higher than the old ITZ. That is, at lower w/c ratio, the old ITZ governs the failure. The lower value of microhardness indicates the higher values of porosity and softness of cement paste. That is, the old ITZ is loose and more porous at lower w/c ratio. Therefore, at lower w/c ratio, the strength of RAC depends on the quality of RCA, as the strength of old ITZ weaker than the strength of new ITZ and at higher w/c ratio, the strength does not depend on the quality of RCA, as the old ITZ is stronger than the new ITZ. Therefore, at higher w/c ratio, the strength of RAC was same as that of normal concrete.

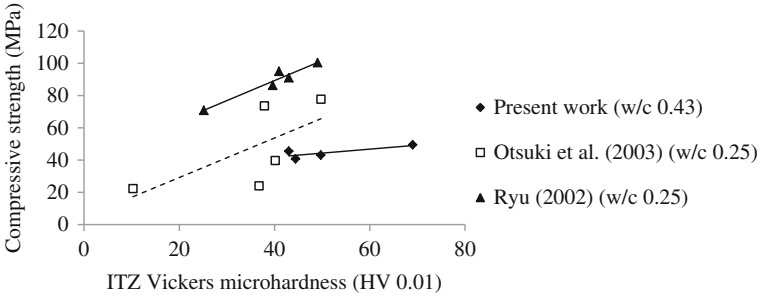

Fig. 6.31 Relationship between compressive strength and ITZ Vickers microhardness (Chakradhara Rao 2010)

The overall performance of the concrete may depend on the quality of RCA i.e. the strength of original concrete from which the recycled aggregate derived and the crushing technology. The concrete produced with recycled coarse aggregate may not differ much with normal concrete with respect to the mechanical characteristics. However, the RCA may influence the durability and long-term properties of concrete such as creep and shrinkage, as more microcracks and high porosity exist in RAC due to the adherence of porous cement paste.

6.11 Influence of Binder on ITZ

Li et al. (2001) studied the influence of different binders, namely pure cement paste binder (C-binder), expansive binder (E-binder), and polymer modified and fly-ash binder (F-binder) on interfacial transition zone (ITZ) between new and old concretes. The microstructure of the transition zone between old concrete (three months) and a new concrete of same mix proportion with the above binders was examined by using H-1030 SEM with EDS analyzer. The mix proportion of the binders is shown in Table 6.5.

The interfacial transition zone was highly dense and uniform and no ettringite or calcium hydroxide was found in the transition zone (Fig. 6.32a) when E-binder was used. This was due to the formation of additional calcium silicate hydrate (C–S–H), when the calcium hydroxide produced by the hydration of cement reacts with the amorphous silica of fly ash in F-binder, fills the pores and the pozzolanic reaction decreases the calcium hydroxide content. Further, a large number of globular particles of fly ash fill the weak spaces of ITZ, which make it highly dense and uniform. In E-binder, the hydration products of U-type expansive agent are the mainly ettringite crystals, which creates more number of microcracks in the

Table 6.5 Mix proportion of binders (Li et al. 2001)

Binder type	Cement	Water	Sand	Fly ash	U-type expansive agent	Supe plasticiser dosage[a]
C-binder	1	0.4	–	–	–	0.5
F-binder	0.75	0.4	1	0.25	–	1.5
E-binder	0.9	0.4	–	–	0.1	0.5
Polymer (YJ-302)	One of the main components of the polymer-modified binder (YJ-302) was emulsified epoxy resin					

[a]Dosage given as percentage of total binder content by mass

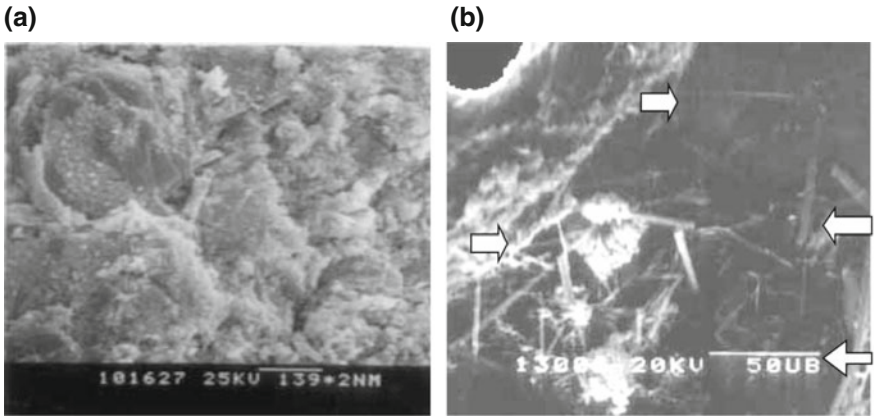

Fig. 6.32 Transition zone with (**a**) F-binder and (**b**) E-binder (Li et al. 2001)

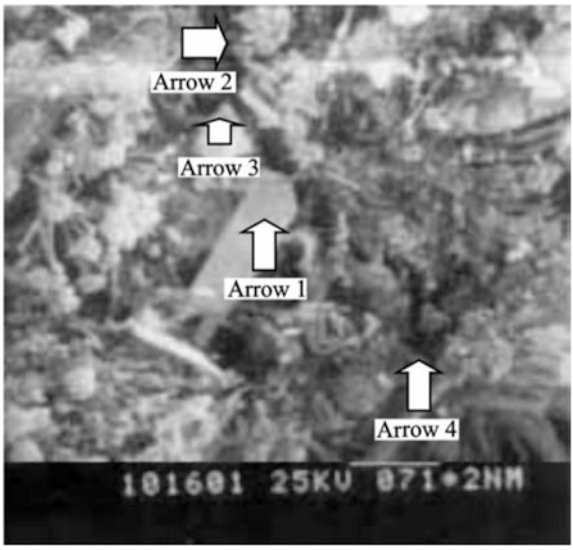

Fig. 6.33 Transition zone with C-binder (Li et al. 2001)

interfacial transition zone (Fig. 6.32b). A large number of microcracks and crystals in the ITZ and interface debond between new to old concrete were found due to drying shrinkage of cement in C-binder (Fig. 6.33). When polymer binder was used near the old concrete surface, only the polymer film was found (Fig. 6.34).

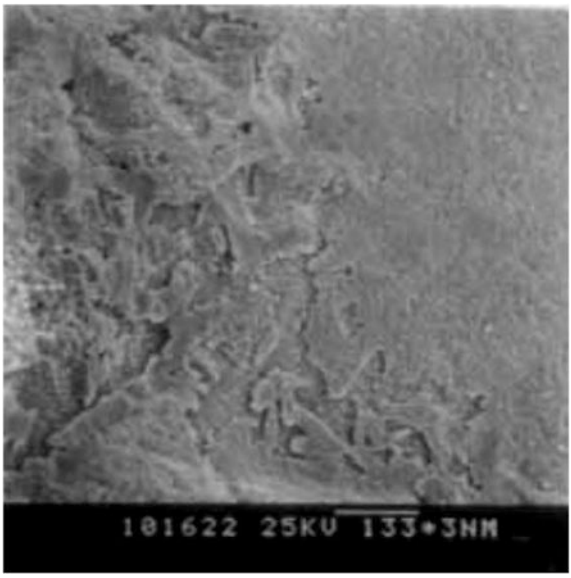

Fig. 6.34 Cross section of interface with polymer binder (Li et al. 2001)

6.12 Influence of the Water–Binder Ratio, Quality and Quantity of Adhesion Mortar

The influence of water–cement ratio (0.25, 0.40, 0.55, 0.70), strength of adhesive mortars, and quantity of adhesive mortars of recycled coarse aggregate (Table 6.6) on the interfacial transition zones of recycled aggregate concrete and natural aggregate concrete are presented in Figs. 6.35, 6.36, 6.37, 6.38, 6.39 and 6.40 (Otsuki et al. 2003). The microhardness was considered as the criterion for characterizing the ITZ. It can be seen from Figs. 6.35 and 6.36 that the Vickers microhardness increased with the decrease in water–binder ratio in both natural

Table 6.6 Details of natural and recycled coarse aggregates (Otsuki et al. 2003)

Symbol	Aggregate type	Adhesive mortar		Specific gravity	Water absorption (%)	Fineness Modulus
		Strength (MPa)	Quantity (%)			
VC	Normal aggregate	–	–	2.66	0.69	6.73
A2	Recycled aggregate	68.5	39.7	2.47	3.58	6.50
B1		51.7	20.8	2.54	2.68	6.45
B2		51.7	44.6	2.44	4.50	6.69
B3		51.7	50.8	2.41	5.13	6.62
C2		32.3	35.0	2.45	4.36	6.46
Original aggregate in recycled aggregate				2.64	0.84	6.68

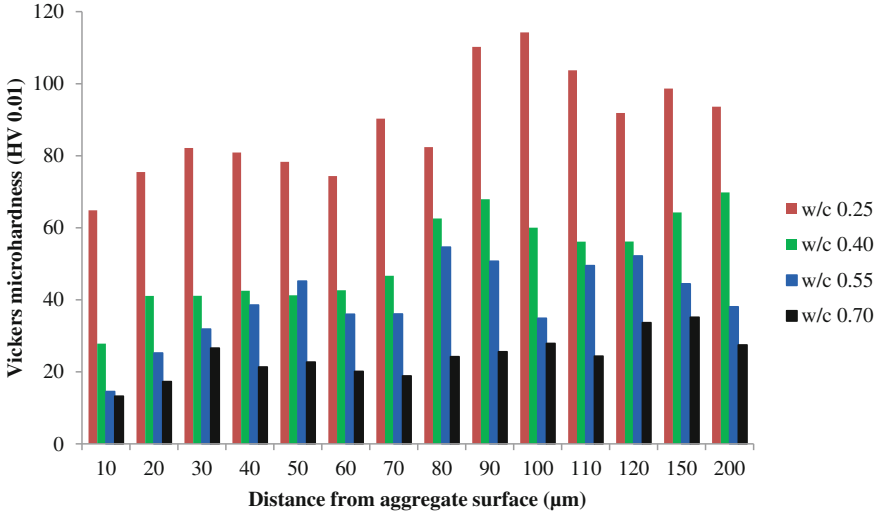

Fig. 6.35 Vickers microhardness distribution at new ITZ of recycled aggregate concrete B2 (Otsuki et al. 2003)

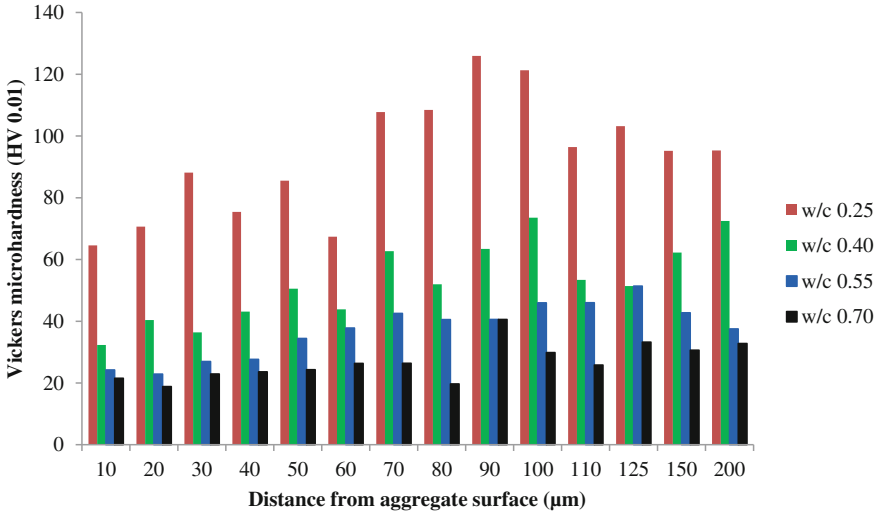

Fig. 6.36 Vickers microhardness distribution at new ITZ of normal aggregate concrete VC (Otsuki et al. 2003)

aggregate concrete and recycled aggregate concrete. Figure 6.37 shows that the Vickers microhardness of old ITZ increased with the increased quality of adhesive mortar, whereas the Vickers microhardness of old ITZ does not change with the quantities of mortar (Fig. 6.38). That means, the characteristics of ITZ depend on

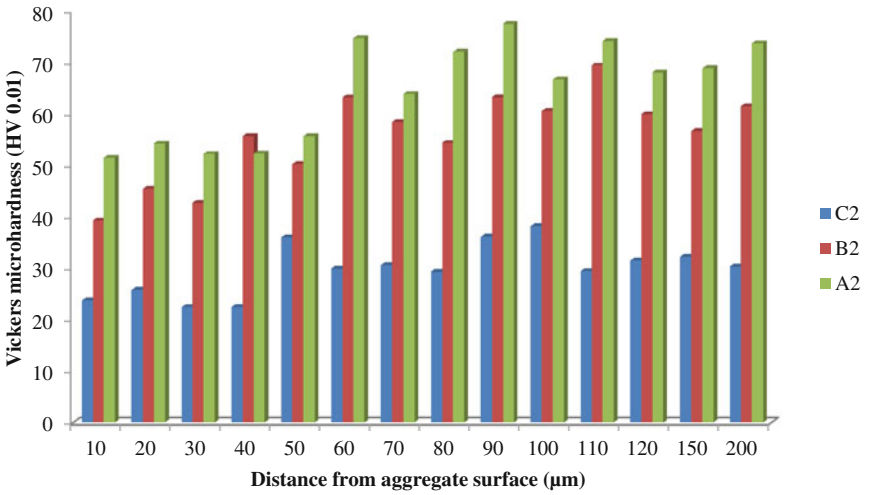

Fig. 6.37 Vickers microhardness distribution at old ITZ of recycled aggregate with different adhesive mortar strengths (*Source* Otsuki et al. 2003)

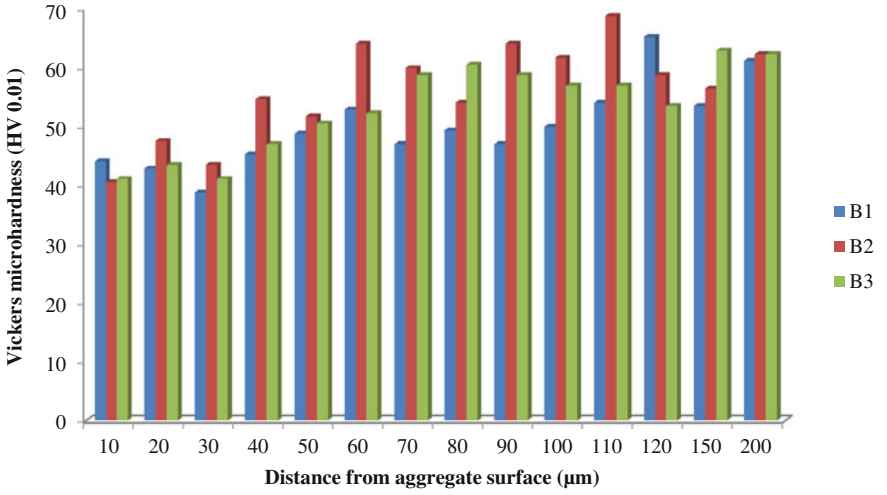

Fig. 6.38 Vickers microhardness distribution at old ITZ of recycled aggregate with different adhesive mortar quantities (*Source* Otsuki et al. 2003)

the quality of mortar surrounding the aggregate and not on the adhered mortar quantity. Figure 6.39 and 6.40 show the Vickers microhardness of old and new ITZ for 0.25 and 0.55 water–binder ratios. It can be seen that at lower water ratio, the new ITZ is stronger than old ITZ, whereas at higher water–binder ratio, the old ITZ

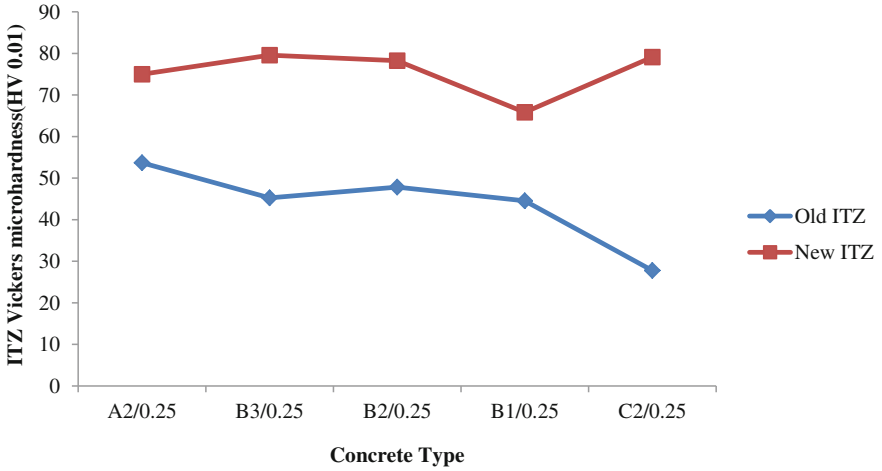

Fig. 6.39 New and old ITZs Vickers Microhardness (w/b 0.25) (*Source* Otsuki et al. 2003)

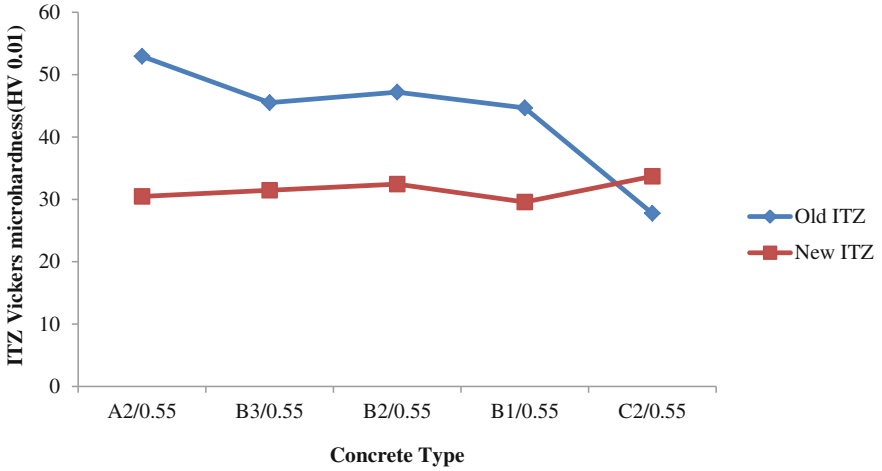

Fig. 6.40 New and old ITZs Vickers microhardness (W/C 0.55) (*Source*: Otsuki et al. 2003)

becomes stronger except in case RAC with C2 type (having lowest strength of adhesive mortar among all types of RA). At lower w/c ratio, the strength of RAC depends on the quality of RCA, and as the strength of old ITZ weaker than the new ITZ and at higher w/c ratio, the strength does not depend on the quality of RCA, as the old ITZ stronger than the new ITZ. Therefore, at higher w/c ratios, the strength of RAC was same as that of normal concrete.

6.13 Influence of Strength of Source Concrete

Influence of natural aggregate and RCA derived from the high performance concrete (HPC) and normal strength concrete (NC) on microstructure of RAC were examined by Poon et al. (2004) are presented in Figs. 6.41, 6.42, and 6.43. It can be seen from Fig. 6.41 that the granite aggregate and cement interface was relatively loose and the interfacial transition zone thickness varied along the aggregate surface. The interfacial transition zone between RCA obtained from normal strength concrete and cement matrix is shown in Fig. 6.42. It was observed that the width of ITZ was approximately 30–60 μm which consists mainly of loose particles (Fig. a). Further, at higher magnification, it can be seen that the ITZ was porous with high porosity (Fig. b). A relatively dense ITZ in RAC made with RCA obtained from HPC was observed (Fig. 6.43). The poor ITZ in RAC with normal strength concrete

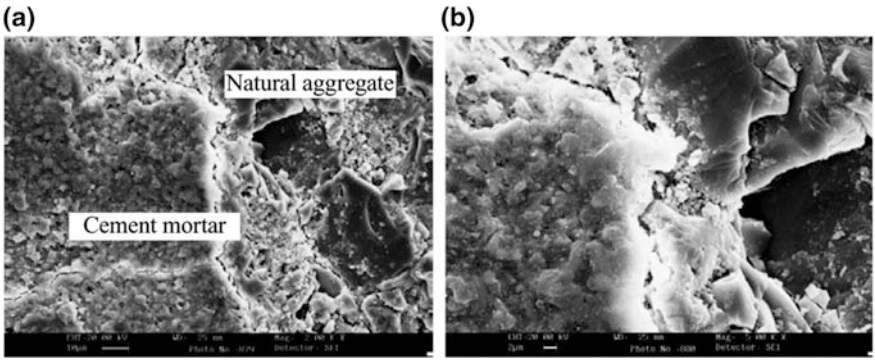

Fig. 6.41 Microstructure of concrete prepared with natural crushed granite (Poon et al. 2004)

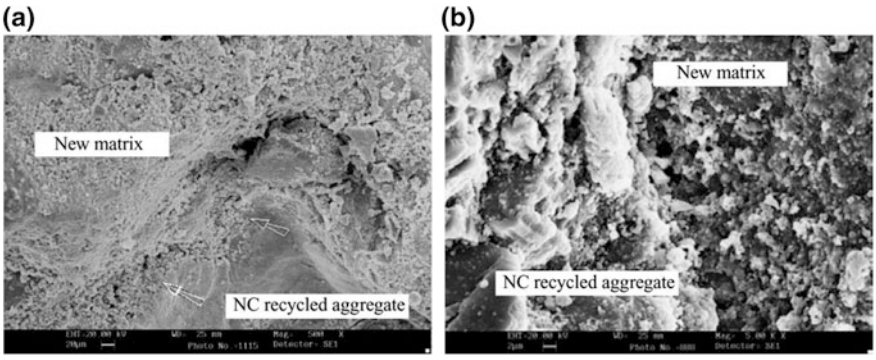

Fig. 6.42 Microstructure of concrete prepared with recycled NC (Poon et al. 2004)

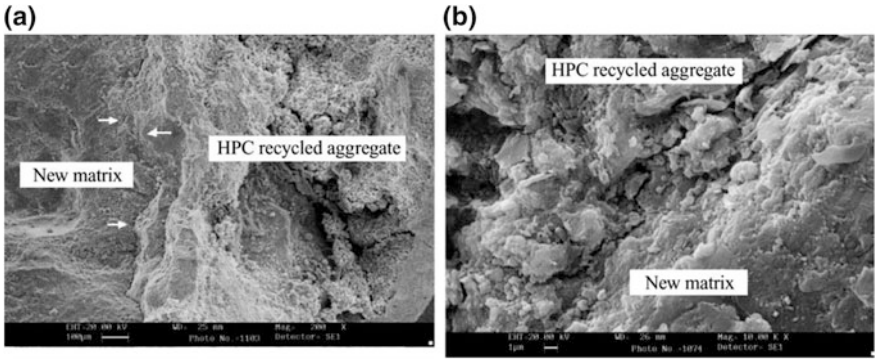

Fig. 6.43 Microstructure of concrete prepared with recycled HPC (Poon et al. 2004)

aggregate attributes to the higher porosity and absorption capacity of recycled aggregate. The ITZ in recycled aggregate concrete is considered to be an important factor in governing the compressive strength development in RAC.

6.14 Influence of Treatment of RCA on ITZ

The quality of ITZ between recycled aggregate and the new cement mortar can be improved by impregnating the recycled aggregate in silica fume solution (Katz 2004). By impregnating the recycled aggregate in silica fume solution, the cracked and loose layer of the recycled aggregate could be filled with silica fume particles. During the hardening of concrete, due to this filler effect, the ITZ improves. In addition, the pozzolanic reaction between the portlandite and the silica fume strengthen the feeble structure of the recycled aggregate to form an improved zone, which extends from the natural aggregate through the residues of the old cement paste into the new cement matrix.

6.15 Summary

The detailed experimental results of the characteristics of interfacial transition zone in both normal concrete and recycled aggregate concrete made with 100% recycled coarse aggregate obtained from three different Sources have been presented. The detailed specimen preparation for microscopic examination, image acquisition, and image analysis techniques along with the brief description of scanning electron microscope and Vickers microhardness instruments is discussed. The important features of ITZ, viz: anhydrous cement, hydration compounds, and porosity are discussed. The strength—porosity and microhardness—porosity relationships are

discussed. Further, the effect of water–cement ratio, strength of adhesive mortars and quantity of adhesive mortars, strength of source concrete and impregnation of RCA in silica fume on the interfacial transition zones were discussed. Based on these discussions, the following key points are noted down.

- The ITZ in RAC is less dense than the concrete with natural aggregates. Possibly, the adhered mortar to the aggregates in RCA consumes more water in the initial stages, thereby making the surrounding more porous.
- The gradients of anhydrous cement and hydration compounds indicate that the width of ITZ is around 40 μm in RAC with different percentages of RCA investigated. However, the porosity gradients indicate that the width of ITZ in RAC is more than the width of ITZ in normal concrete. In addition to the high absorption capacity of RCA stated above, the total aggregate–cement ratio also influences the width of ITZ.
- The Vickers microhardness of ITZ in RAC is lower than that of normal concrete. Lower values of microhardness indicate the presence of more microcracks and micropores, which are indication of higher porosity. Possibly, this makes the concrete less dense and lower stiffness.
- The compressive strength of concrete decreases with the decrease in microhardness and increase in porosity of ITZ.
- The type of binder influences the characteristics of ITZ. Among the three binders, namely pure cement paste binder (C-binder), expansive binder (E-binder), and polymer modified and fly-ash binder (F-binder), the ITZ was highly dense and uniform when F-binder was used.
- The characteristic of ITZ depends on the quality of mortar surrounding the aggregate and not on the adhered mortar quantity.
- At lower w/c ratio, the strength of RAC depends on the quality of RCA, as the strength of old ITZ weaker than the new ITZ, and at higher w/c ratio, the strength does not depend on the quality of RCA, as the old ITZ stronger than the new ITZ.
- The strength of source concrete influences the ITZ. ITZ was relatively dense in RAC made with RCA obtained from HPC than that made with RCA from normal strength concrete.

References

Chakradhara Rao M (2010) Characterisation and behaviour of recycled aggregate concrete. Ph.D. Thesis, Indian Institute of Technology Kharagpur, West Bengal, India

Crumbie A K (1994) Ph.D. Thesis, University of London

Diamond S (2001) Considerations in image analysis as applied to investigations of ITZ in concrete. Cem Concr Comp 23:171–178

Diamond S (2004) The microstructure of cement paste and concrete—a visual primer. Cem Concr Comp 26:919–933

Diamond S, Huang J (2001) The ITZ in concrete—a different view based on image analysis and SEM observations. Cem Concr Comp 23:179–188
Igarashi S, Bentur A, Mindess S (1996) Microhardness testing of cementitious materials. Adv Cem Based Mater 4:48–57
Katz A (2004) Treatments for the improvement of recycled aggregate. J Mater Civ Engg ASCE 16:597–603
Li G, Xie H, Xiong G (2001) Transition zone studies of new-to-old concrete with different binders. Cem Concr Comp 23:381–387
Mehta PK, Monterio PJM (2006) Concrete (microstructure, properties and materials). Prentice-Hall, Englewod Cliffs
Neville AM (2006) Properties of concrete. Pearson Education Ltd
Otsuki MN, Shin-Ichi M, Wanchai Y (2003) Influence of recycled aggregate on interfacial transition zone, strength, chloride penetration and carbonation of concrete. J Mater Civ Engg ASCE 15:443–451
Poon CS, Shui ZH, Lam L (2004) Effect of Microstructure of ITZ on compressive strength of concrete prepared with recycled aggregates. Constr Build Mater 18:461–468
Ryu JS (2002) An experimental study on the effect of recycled aggregate on concrete properties. Mag Concr Res 54:7–12
Sahu S, Badger N, Thaulow N, Lee RJ (2004) Determination of water—cement ratio of hardened concrete by scanning electron microscopy. Cem Concr Comp 26:987–992
Scrivener KL (2004) Backscattered electron imaging of cementitious microstructures: understanding and quantification. Cem Concr Comp 26:935–945
Scrivener KL, Pratt P (1996) Characterisation of interfacial microstructures. In: Maso J. C. (ed) Interfacial transition zone in concrete, State of the Art report, RILEM Committee 108 ICC, FN. Spon, London, 3–17
Scrivener KL, Crumbie AK, Laugesen P (2004) The interfacial transition zone (ITZ) between cement paste and aggregate in concrete. J Inter Sci 12:411–421
Tasong WA, Lynsdale CJ, Cripps JC (1998) Aggregate-cement paste interface: influence of aggregate physical properties. Cem Concr Res 28:1453–1465
Tasong WA, Lynsdale CJ, Cripps JC (1999) Aggregate-cement paste interface Part I. influence of aggregate geochemistry. Cem Concr Res 29:1019–1025